POLISH MARITIME RESEARCH 3 (119) 2023 Vol. 30; pp. 163-173
10.2478/pomr-2023-0049

RESEARCH ON THE MODIFIED ECHO HIGHLIGHT MODEL FOR UNDERWATER VEHICLES WITH COMBINED STRUCTURES

Xin Xie [1]
Fanghua Liu [1]
Guangwen Jin [2]
Jinwei Liu [3]
Cong Xu [3]
Zilong Peng [4*]

[1] School of Mechanical Engineering, Jiangsu University of Science and Technology, Zhenjiang, Jiangsu 212100, China
[2] Shanghai Marine Equipment Research Institute, Shanghai 200031, China
[3] School of Energy and Power, Jiangsu University of Science and Technology, Zhenjiang, Jiangsu 212100, China
[4] Jiangsu University of Science and Technology, Zhenjiang, China,

* Corresponding author: *zlp_just@sina.com (Zilong Peng)*

ABSTRACT

The highlight model is widely used as a simple and convenient method in the radar field but its accuracy is not high. Based on the traditional highlight model, the algorithm has been improved to address the acoustic scattering problems of underwater vehicles with more complex line shapes. The basic idea is to partition the model into micro-bodies to calculate the scattered sound pressure, consider the phase interference of each part, and then synthesise the scattered sound pressure to approximate the target's actual shape. A computational model of the wedge-shaped convex structure on the back of the underwater vehicles is developed using a highlight model of a trapezoidal plate. The results of the calculations using the highlight model approach are consistent with those of the planar element method. Utilising the modified highlight model method, the accuracy of acoustic scattering characteristics calculations for the stern and overall structures of underwater vehicles has proven satisfactory. Finally, fast acoustic scattering prediction software is developed for underwater vehicles, enabling the calculation of the acoustic scattering characteristics for individual structures, combined structures, and coated silent tiles. This software provides algorithmic support for the fast prediction of the acoustic stealth performance of underwater vehicles.

Keywords: modified highlight model, wedge-shaped convex structure, piecewise synthesis method, acoustic scattering calculation software

INTRODUCTION

Predicting the acoustic scattering of complex underwater targets is an important research direction in modern hydroacoustics. The characteristics of target acoustic scattering serve as a crucial foundation for active sonar in detecting and recognising underwater targets [1]. The methods for studying the acoustic scattering characteristics of underwater targets can be categorised as either numerical or approximate methods. Among the numerical methods, the Rayleigh normal mode solution [2,3] is primarily used to predict the acoustic scattering characteristics of simple targets; the integral equation method [4-6] can lead to singularities in the integral equation or uniqueness of the solution; the finite element/boundary element method [7-10] is suitable for small-sized targets at low frequencies; and the T-matrix method [11,12] exhibits low computational efficiency. The approximation method is mainly employed for high-frequency problems. Lee and Seong [13] derived a time-domain solution of the impedance polygon facet from the Kirchhoff formula. Fan and Tang [14–16] introduced the Planar Elements Method, which they continuously modified. Abawi [17] developed a method for solving both frequency-domain and time-domain solutions for arbitrarily shaped scattered sound fields, based on the Kirchhoff approximation.

Stanton [18,19] proposed the deformed cylinders method, building upon the concept of a radiating sound field from an inhomogeneous line source. Tang [20] proposed the highlight model after summarising research results on target acoustic scattering, describing the highlight characteristics with three parameters: amplitude, time delay, and phase factors. Theoretical analysis and experimental results demonstrate that, in the case of high frequency, complex targets can be represented as combinations of several highlights, each producing an echo. The total echo results from the interference superposition of these highlight echoes. Liu [21] and Chen [22] conducted investigations into the echo highlight of complex targets. In the present study, the highlight model is utilised to calculate the echoes of the complex underwater vehicles model, but it exhibits limited accuracy in the target echoes.

In this paper, we modified the highlight model by utilising the piecewise synthesis method [23,24] to further enhance the computational accuracy of the highlight model. The modified highlight method was employed to calculate the acoustic scattering characteristics of the wedge-shaped convex structure and several sub-structures of the underwater vehicles. The results were compared with those of the planar element method and they showed relatively consistent findings. Finally, based on the theoretical work, we summarised the highlight model method and developed two software programs: 'Target Strength Prediction Software for Simple Convex Structure of Underwater Vehicles' and 'Target Strength Fast Prediction Software for Multi-Highlight Interference of Underwater Vehicles'.

HIGHLIGHT MODEL FOR ACOUSTIC SCATTERING FROM A FINITE ELLIPTICAL CYLINDER

The shape of the sail and rudder of early underwater vehicles is similar to that of an elliptical cylinder, making them suitable for approximation using the scattering highlight of an elliptical cylinder, as depicted in Fig. 1. We employed the physical acoustic method and the saddle point approximation method to derive two equivalent edge highlights for the upper and lower edges of the elliptical cylinder, resulting in the transfer function [25]:

$$H(\vec{r},\omega) = H_1(\vec{r},\omega) + H_2(\vec{r},\omega) \tag{1}$$

$$H_1(\vec{r},\omega) = \frac{C}{D} e^{2jk\left(\sqrt{(Aa)^2+(Bb)^2} + L\cos\theta\right)-j\frac{5\pi}{4}} \tag{2}$$

$$H_2(\vec{r},\omega) = \frac{C}{D} e^{2jk\left(\sqrt{(Aa)^2+(Bb)^2} + L\cos\theta\right)-j\frac{\pi}{4}} \tag{3}$$

where $A = \sin\theta\cos\varphi$, $B = \sin\theta\sin\varphi$, $C = ab(A^2+B^2)$, and $D = 4\sqrt{k\pi}\cos\theta\left((Aa)^2+(Bb)^2\right)^{3/4}$.

When $a = b$, Eq. (1) represents the highlight transfer function for a finite cylinder.

We further calculated the target strength for an elliptical cylinder with dimensions $a = 3$ m, $b = 1$ m, and $L = 5$ m, using the highlight model method and the planar element method, respectively, in the frequency band of 1-10 kHz; the results are depicted in Fig. 2.

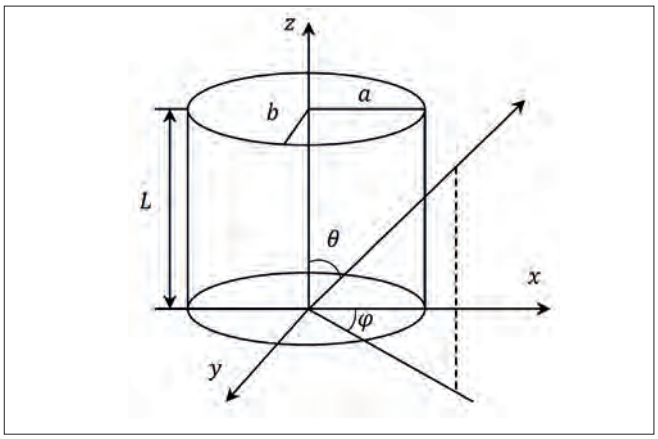

Fig. 1. Geometry of the elliptical cylinder

SIMPLE STRUCTURAL HIGHLIGHT MODEL METHODOLOGY AND VALIDATION

The underwater vehicles have a bulged back structure [26], which can be seen as a stretched trapezoidal plate, usually behind the sail or as a whole, filled above the hulling cylinder. The convex sides and top of the structure are similar to a plate, so a trapezoidal plate structure can be used as an approximate substitute, as depicted in Fig. 3.

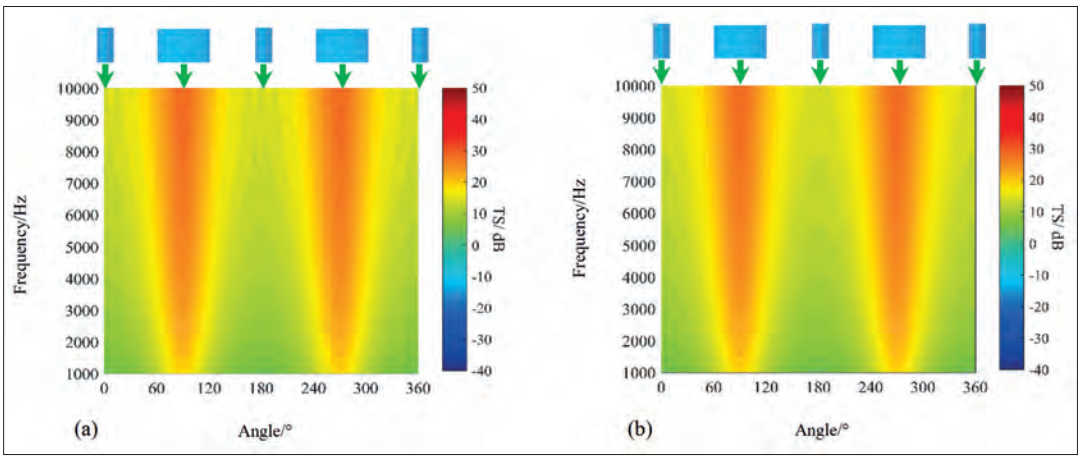

Fig. 2. Echo characteristics of finite elliptical cylinder a) planar element method b) highlight model method

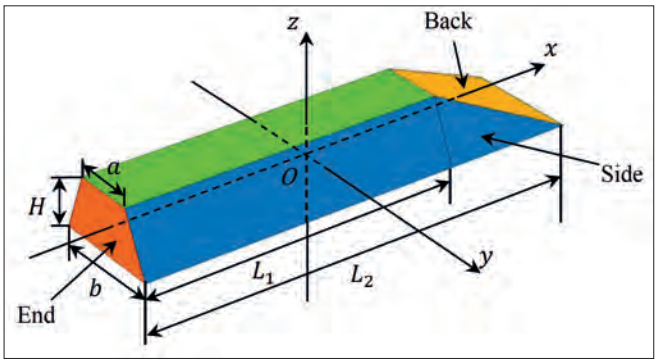

Fig. 3. 3D model of wedge-shaped structure

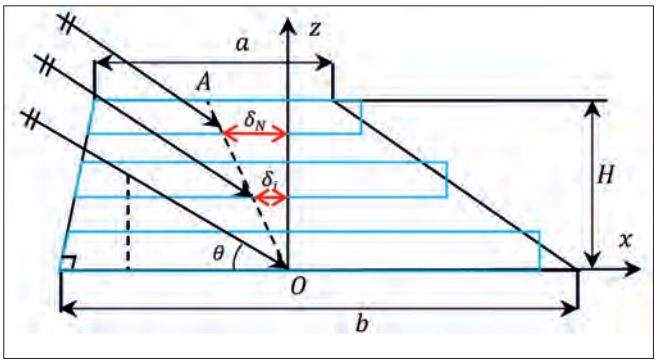

Fig. 4. Schematic diagram of the calculation of the highlight model of a right-angle trapezoidal plate

RIGHT-ANGLE TRAPEZOIDAL PLATE HIGHLIGHT MODEL

For a rectangular plate, the four edges produce four highlights when the sound waves are obliquely incident to the plate, and so the transfer function of the rectangular plate is [1]:

$$I = ab\cos\theta \frac{\sin(ka\sin\theta\cos\varphi)}{ka\sin\theta\cos\varphi} \frac{\sin(kb\sin\theta\sin\varphi)}{kb\sin\theta\sin\varphi} \quad (4)$$

When $\varphi = 0°$, the transfer function simplifies to:

$$I = ab\cos\theta \frac{\sin(ka\sin\theta)}{ka\sin\theta} \quad (5)$$

A right-angled trapezoidal plate can be regarded as an isosceles trapezoidal plate with the centre of the upper edge (point A in Fig. 4) shifted by l with respect to the origin O. Right-angled edges are common edges in a micro-rectangular plate. The eccentricity equation $y = f(x)$ is obtained by connecting the centres of the upper and lower edges. The reference point for the phase difference calculation is the origin O, the centre of the side length of the micro-rectangular plate is the intersection of the lower edge of the micro-trapezoidal plate and the equation $y = f(x)$; the distance δ_i between the intersection and the origin O is the phase distance.

Assuming a transfer function of I_i for a micro-rectangular plate, the transfer function, after considering the phase, is:

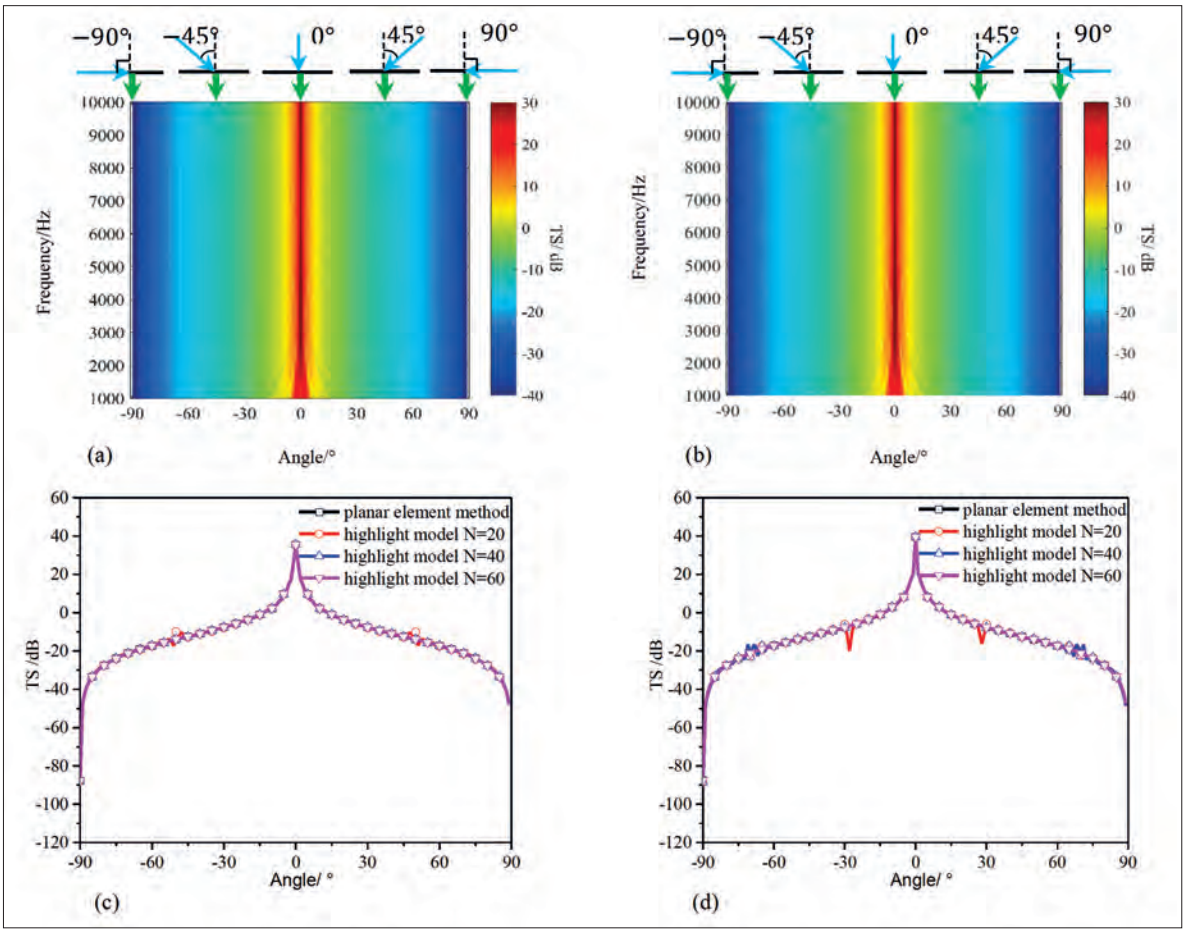

Fig. 5. Computational results comparison: a) planar element method b) highlight model method (=60) c) Target strength curve at 5 kHz d) Target strength curve at 8 kHz

$$\begin{cases} I_1' = I_1 e^{-2jk\delta_1 \sin\theta} \\ I_2' = I_2 e^{-2jk\delta_2 \sin\theta} \\ I_3' = I_3 e^{-2jk\delta_3 \sin\theta} \\ \cdots \\ I_N' = I_N e^{-2jk\delta_N \sin\theta} \end{cases} \quad (6)$$

The equation for calculating the target strength of a right-angled trapezoidal plate is:

$$TS = 10\lg\left(\left|\Sigma_{i=1}^{N} I_i'\right| / \lambda\right)^2 \quad (7)$$

Tab. 1. Computing time for the angular-frequency spectrum

	Planar element	Highlight model
mesh quantity / pcs	538	$N = 60$
Time / s	16.334	2.480

We further calculated the target strength for a right-angled trapezoidal plate with an upper edge of a = 4 m, lower edge of b = 8 m and height of H = 3 m, using the planar element method and the highlight model method in the frequency band of 1-10 kHz. The results are presented in Fig. 5 and the time required for the two calculation methods is presented in Table 1.

SIDE PLATE HIGHLIGHT MODEL

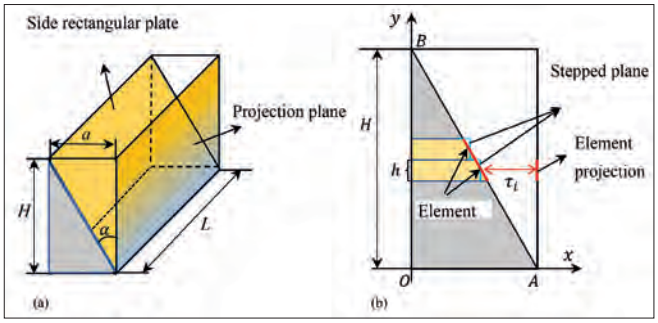

Fig. 6. Local model schematic diagram a) 3D view b) front view

Fig. 6 shows that the normal direction of the side plate is not in the coordinate plane, so the side plate needs to be further divided and approximated. For a certain angle α between the side plate and the projection plane, the projection plane is parallel to the *xoz* plane and the projection plane is used as a reference for the calculation of phase differences.

If the side plate in the *OB* direction is segmented and the divided inclined plane is projected into the projection plane, an inclined plane is equivalent to a stepped plane, as shown in Fig. 6(b). The height of any section of the projection plane is $h = H/N$, the distance between the stepped plane and the projection plane is the sound path difference, and the sound path difference τ_i is:

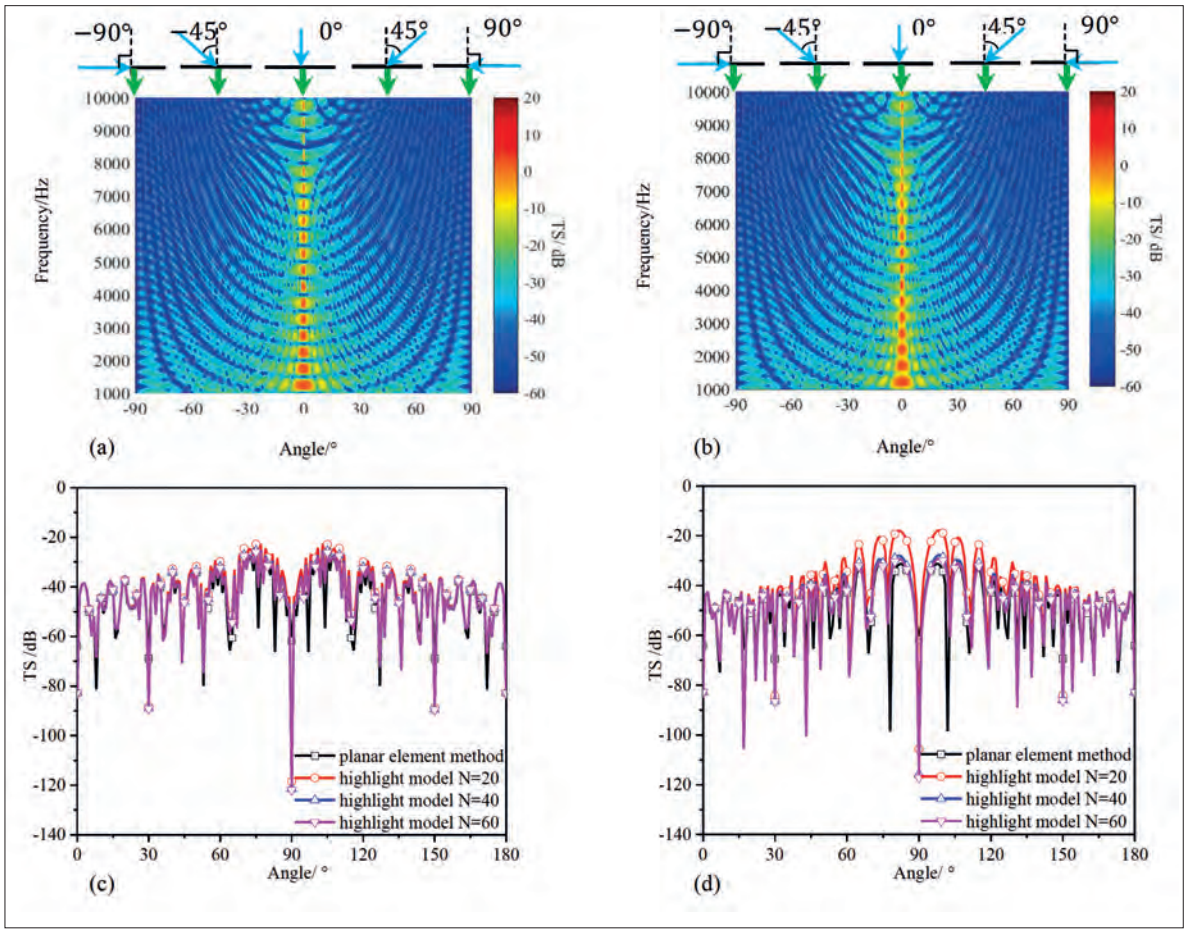

Fig. 7. Computational results comparison a) planar element method b) highlight model method (=60) c) Target strength curve at 5 kHz d) Target strength curve at 8 kHz

$$\tau_i = L_{OA} - y^{-1}(x_i) \tag{8}$$

L_{OA} is the distance between point O and point A, $y^{-1}(x_i)$ is the x-coordinate of the line equation $y(x)$ between A and B, and x_i is the x-coordinate of the intersection between the midpoint of each inclined plane height and the function $y(x)$.

The tilt of each inclined plane is described by the sound path difference τ_i between each inclined plane and its projection. Let the transfer function of any stepped plane be I_i, and the transfer function, considering the sound path difference τ_i, is:

$$I_i^1 = I_i e^{2jk\tau_1 \cos\theta} \tag{9}$$

So the transfer function of the side plate is:

$$I_i^2 = I_i^1 e^{2jk\tau_1 \cos\theta} e^{2jk\delta_i \sin\theta} \tag{10}$$

We further calculated the target strength of a side plate with $a = 1.5$ m, $H = 3$ m and $L = 5$ m using the planar element method and the highlight model method, respectively, for the frequency band 1-10 kHz. The results are presented in Fig. 7 and the time required for the two calculation methods is presented in Table 2.

Tab. 2. Computing time for the angular-frequency spectrum

	Planar element	Highlight model
mesh quantity / pcs	227	$N = 60$
Time / s	15.937	1.749

The results in Figs. 5 and 7 show that:

(1) There is strong agreement between the results obtained through the highlight model method and the planar element method, in terms of key features;
(2) When the calculation frequency increases, the number of segments N also needs to be increased appropriately;
(3) The angular-frequency spectrum of the acoustic target strength and the variation curve of the target strength, calculated using the highlight model method, are consistent with the results of the planar element method.

Therefore, the combinations of a rectangular plate can be used to approximate the highlight parameters of a trapezoidal plate and an inclined rectangular plate.

VALIDATION OF THE WEDGE-SHAPED STRUCTURE HIGHLIGHT MODEL METHOD

The previous section is the basis for modelling the highlight model of the wedge-shaped structure. The geometric parameters of the wedge-shaped structure are the upper edge of the end panel $a = 1$ m, the lower edge $b = 1.8$ m, and the heights $H = 1$ m, $L_1 = 5$ m, $L_2 = 7$ m. The acoustic wave is incident along the negative direction of the x-axis, the sound target strength is calculated using the planar element method and the highlight model method, respectively; the

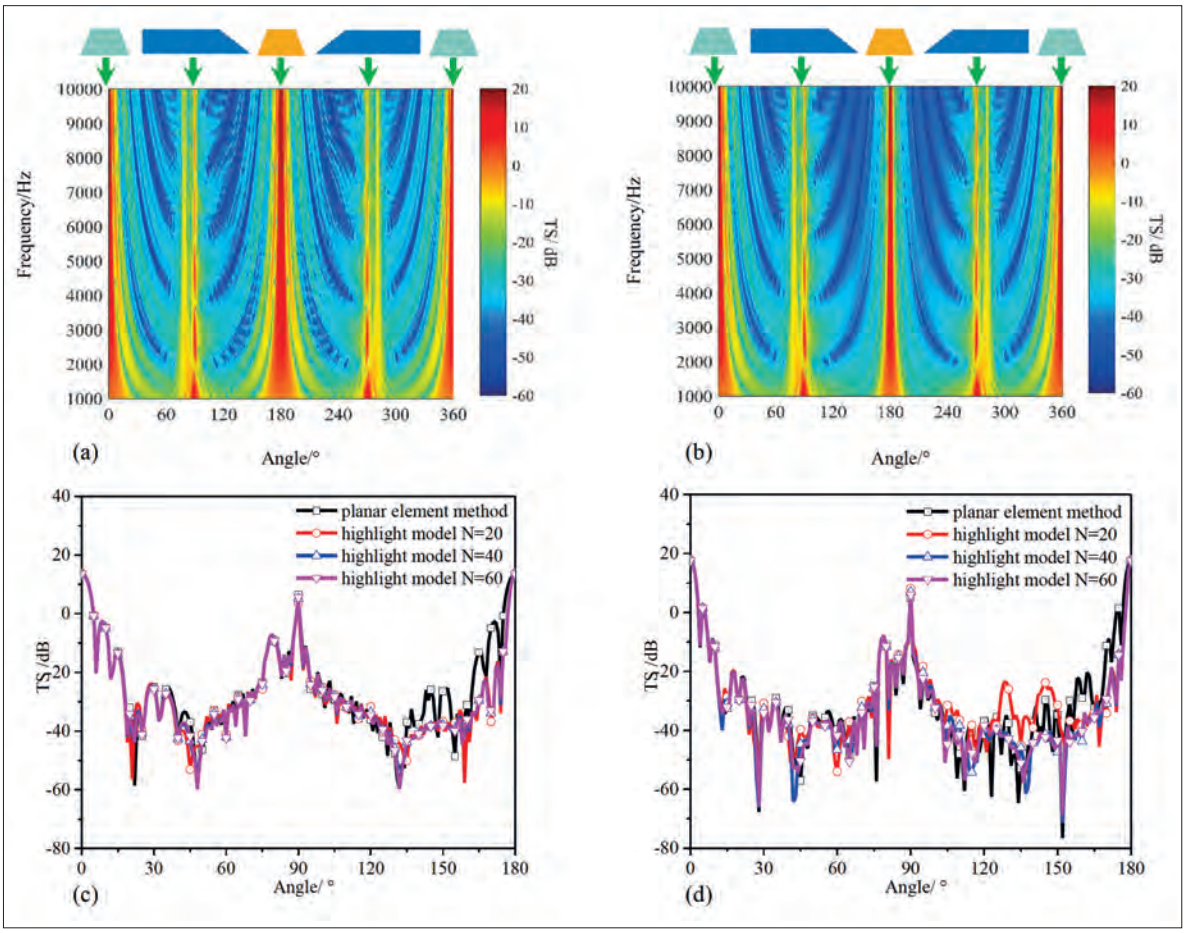

Fig. 8. Computational results comparison a) planar element method b) highlight model method (=60) c) Target strength curve at 5 kHz d) Target strength curve at 8 kHz

calculated frequency band is 1-10 kHz, the calculation results are presented in Fig. 8, and the time required by the two calculation methods is presented in Table 3.

Tab. 3. Computing time for the angular-frequency spectrum

	Planar element	Highlight model
mesh quantity / pcs	938	$N = 60$
Time / s	15.654	6.923

(1) Choosing the appropriate segments N in the range 0-90° can bring the results of the modified highlight model method calculations into high agreement with those of the planar element method.
(2) The calculation results of the highlight model method can reflect the influence of the wedge-shaped structure on the highlight echoes. The low amplitude of the target strength at some frequency points is due to inaccurate phase calculations between the back plate, the end plate, and the side plate.

VALIDATION OF THE STERN STRUCTURE HIGHLIGHT MODEL

The generatrix of the hull stern model is determined by Eq. (11) [27]. To obtain micro-element targets, the model was evenly segmented along the x-axis direction, as depicted in Fig. 9. The radius of the bottom surface of each elliptical truncated cone can be found by substituting the abscissa of the bottom surface into the function $y = f(x)$. This allows us to establish the transfer function of any elliptical truncated cone $H_i(\vec{r},\omega)$. Since changes in the computing centre can lead to phase variations and highlight interference phenomena, we utilise coherent superposition to combine the transfer function and calculate the scattered sound pressure or target strength of the model. The transfer function of the elliptical truncated cone is described by Eq. (12).

$$y = 0.5d - \left(\frac{1.45d}{c^2} - \frac{\tan\theta}{c}\right)(x - c + 0.5L)^2 - \left(\frac{d}{c^3} - \frac{\tan\theta}{c^2}\right)(x - c + 0.5L)^3 \quad (11)$$

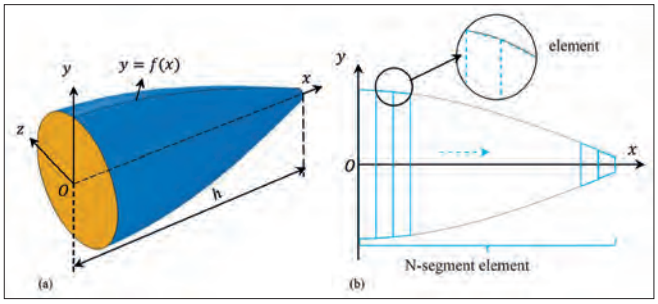

Fig. 9. A rotating body structure with convex smooth generatrix a) 3D model b) Division diagram

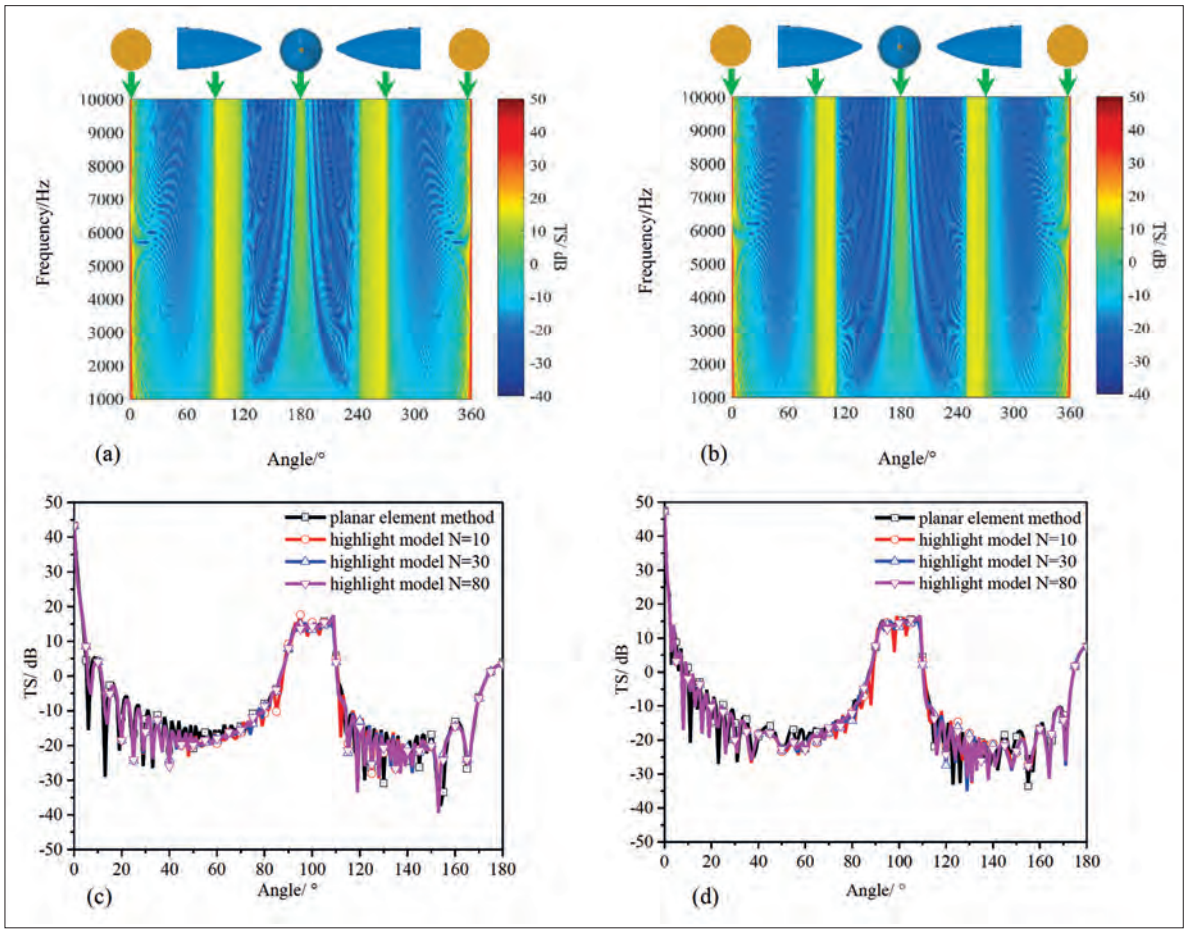

Fig. 10. Computational results comparison a) planar element method b) highlight model method (=80) c) Target strength curve at 5 kHz d) Target strength curve at 8 kHz

$$\begin{cases} H_1'(\vec{r},\omega) = H_1(\vec{r},\omega)e^{-2jk(L_1)\cos(\theta)} \\ H_2'(\vec{r},\omega) = H_2(\vec{r},\omega)e^{-2jk(L_2+h_O)\cos(\theta)} \\ H_3'(\vec{r},\omega) = H_3(\vec{r},\omega)e^{-2jk(L_3+2h_O)\cos(\theta)} \\ \cdots \\ H_N'(\vec{r},\omega) = H_N(\vec{r},\omega)e^{-2jk(L_N+(N-1)h_O)\cos(\theta)} \end{cases} \quad (12)$$

where $H_i'(\vec{r},\omega)$ is the transfer function of the i-segment elliptical truncated cone with respect to the 1-segment elliptical truncated cone; and L_1, L_2, L_3,..., L_N denotes the height of the elliptical truncated cone.

The highlight transfer function of a convex body structure is obtained by using the coherent superposition method, and the target strength calculation is:

$$TS = 10\lg(|\Sigma_{i=1}^{N} H_i'(\vec{r},\omega)|^2) \quad (13)$$

By orienting the large bottom surface at 0° and the small bottom surface at 180°, we calculated the target strength using the planar element method and the highlight model method, respectively. The calculated incidence angle ranges from 0-360° and the calculation frequency band is 1-10 kHz. The calculated results are presented in Fig. 10.

(1) The graph shows that the calculation results of both methods are highly consistent. In addition, with the increase of N, the target of the combination of micro elliptical truncated cones will be closer to the original target and the accuracy of the calculation increases.
(2) In theory, as N increases, the higher the accuracy of the calculation but, in practice, there is an upper limit to the accuracy of the calculation. The number of segments N is too large and affects the efficiency of the calculation. The value of N is related to the calculation frequency and the generatrix type.

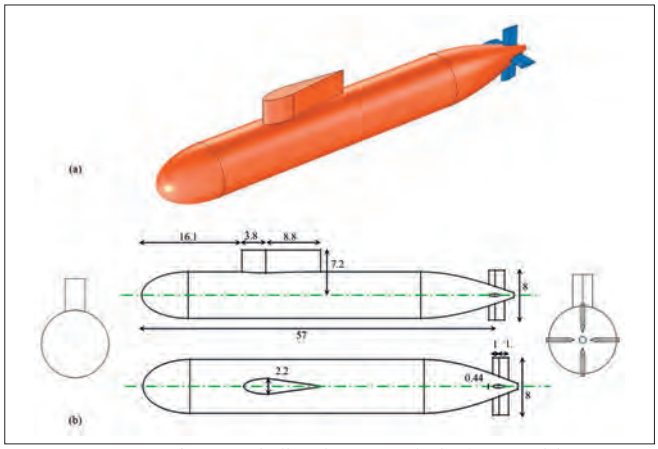

Fig. 11. The mono-hull underwater vehicle a) 3D model b) geometric parameter schematic

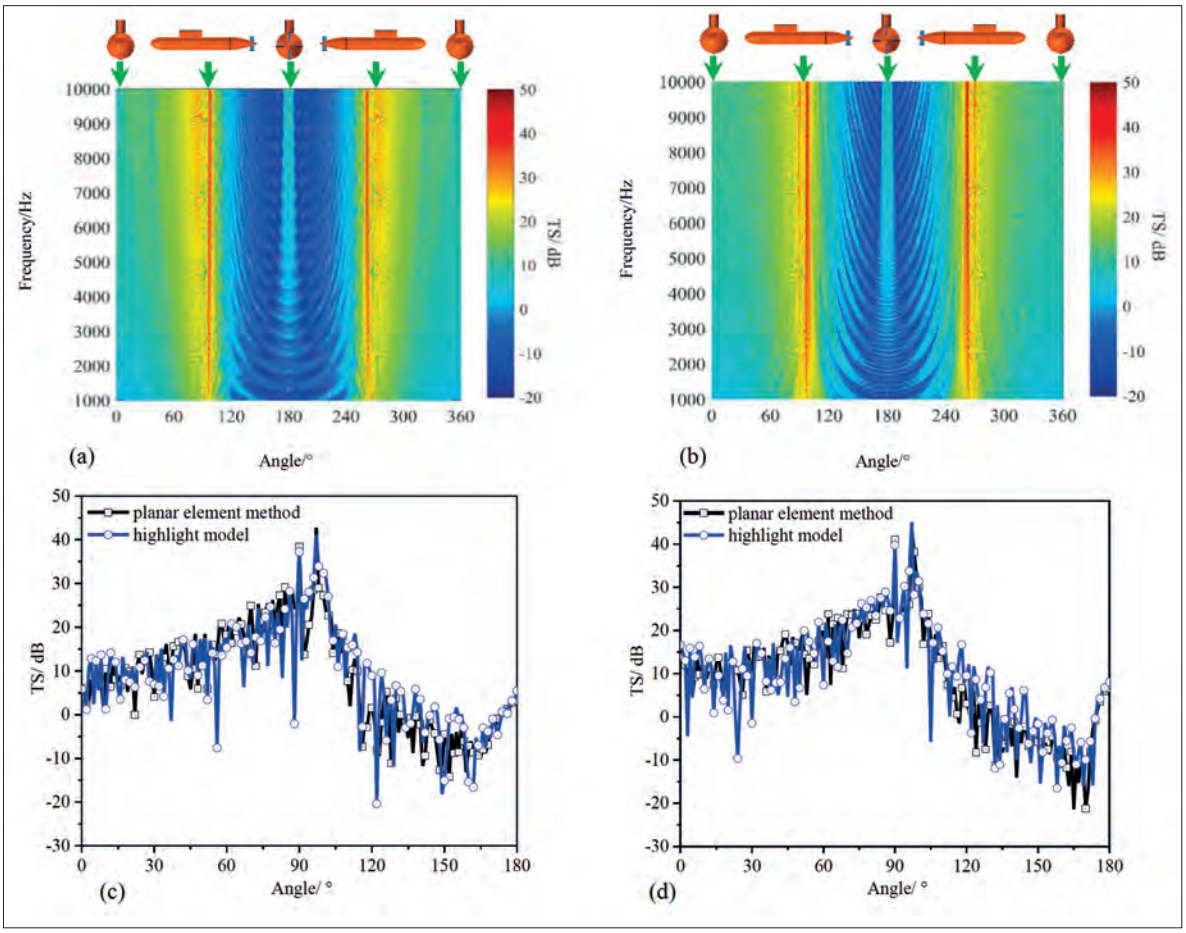

Fig. 12. Computational results comparison a) planar element method b) highlight model method (=100) c) Target strength curve at 5 kHz d) Target strength curve at 8 kHz

VALIDATION OF A HIGHLIGHT MODEL FOR ACOUSTIC SCATTERING FROM MONO-SHELL UNDERWATER VEHICLES

The 3D model of the mono-shell underwater vehicle under study is illustrated in Fig. 11(a) and its geometric parameters are detailed in Fig. 11(b). In this model, the shape of the cross rudder is the same as that of the sail and its geometric parameters are configured based on the rudder of the Benchmark underwater vehicles model, which was adjusted to 8 m.

The planar element method and the highlight model component method were used to calculate the target strength of a mono-shell underwater vehicle. The calculation results are presented in Fig. 12.

Tab. 4. Computing time for the angular-frequency spectrum

	Planar element method	Highlight model method
mesh quantity / pcs	21120	N = 00(stern)
Time / s	118.494	14.386

(1) The highlight model component method, which considers phase, can effectively predict the scattered sound field of large, complex underwater targets and has some engineering applications.

(2) In the range 0-90°, the target strength changes greatly due to the increase in the calculation frequency; there is a strong interference phenomenon between the highlights of each component due to the phase difference. Between 90-180°, the calculation results of the highlight model component method are slightly higher than those of the planar element method because the sail contributes significantly to the scattered sound field of the underwater vehicles.

(3) The calculation time of the highlight model component method is only 14.386 seconds, which is about 8.5 times faster than the planar element method.

RESEARCH ON THE DEVELOPMENT OF FAST-PREDICTION SOFTWARE FOR ACOUSTIC SCATTERING CHARACTERISTICS OF UNDERWATER VEHICLES

By integrating the highlight model of underwater vehicle sub-structures, utilising the traditional highlight model and a modified version of it, we developed two software applications: 'Target Strength Prediction Software for Simple Convex Structure of Underwater Vehicles' and 'Target Strength

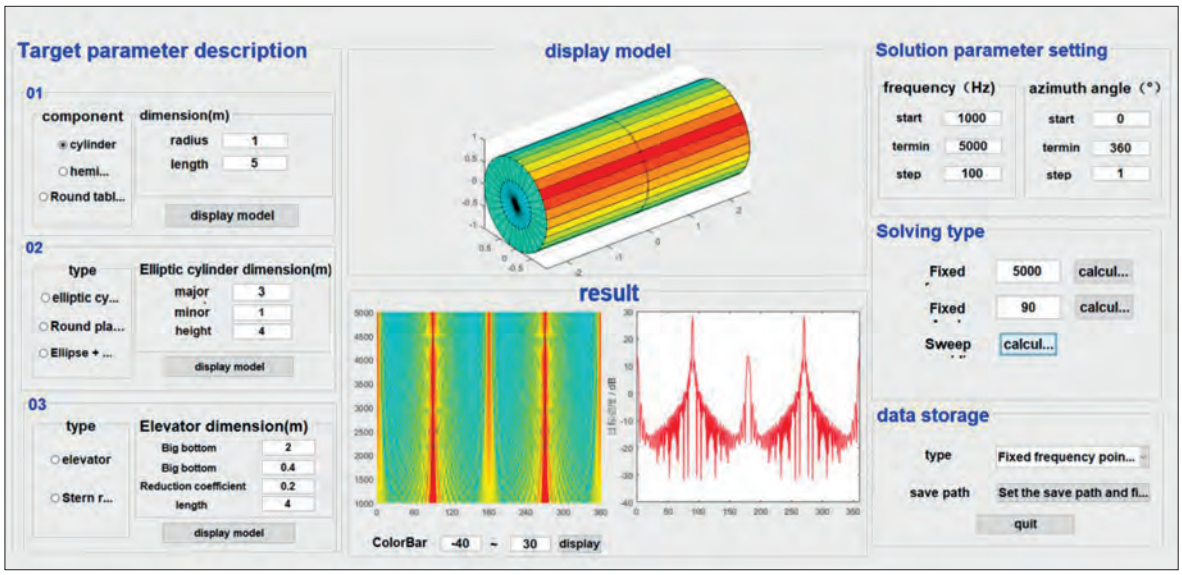

Fig. 13. Software demonstration interface

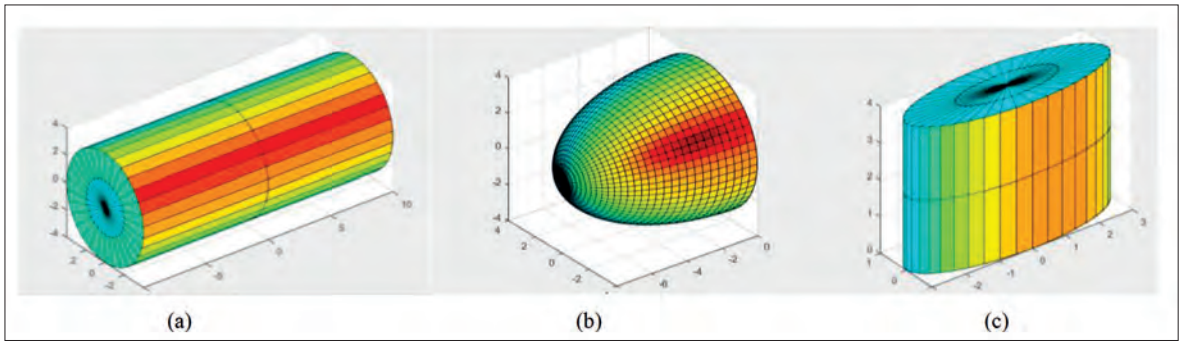

Fig. 14. The modelling results a) Hull Cylinder b) Bow of the hull c) Elliptic cylinder

Fast Prediction Software for Multi-Highlight Interference of Underwater Vehicles'. These software tools were created using the 'MATLAB GUI' platform and were primarily designed for predicting the scattered sound field of the main convex bodies, their attachment structures on underwater vehicles, and the scattered sound field of bare shells or coated silent tiles on mono-shell or double-shell underwater vehicles, as well as mono-shell and double-shell hybrid underwater vehicles.

TARGET STRENGTH PREDICTION SOFTWARE FOR SIMPLE CONVEX STRUCTURES OF UNDERWATER VEHICLES

The demonstrative interface of the software is exhibited in Fig. 13, which can be divided into three main functional areas:

(1) Calculation object selection area: According to the main components of underwater vehicles, the target can be divided into 'hull', 'superstructure' and 'rudder' components, each of which can be further divided into different sub-targets. Fig. 14 shows a few of the modelling results.
(2) Calculation parameter setting area: The main function of this section is setting parameters, such as calculation frequency and angle, but also post-processing modules.
(3) Display area for calculation results: The main function of this section is to display the modelling results and calculation results.

TARGET STRENGTH FAST PREDICTION SOFTWARE FOR MULTI-HIGHLIGHT INTERFERENCE OF UNDERWATER VEHICLES

Software introduction

The software interface of the 'Target Strength Fast Prediction Software for Multi-Highlight Interference of Underwater Vehicles' contains a modelling window, defining acoustic coverage layer window, modelling visualisation window, defining calculation parameter window, calculation result viewing window, and post-processing window, as shown in Fig. 15. The interface specifically includes the following major sections:

(1) Modelling section: a mono-shell underwater vehicles model, double-shell underwater vehicles model, and mono-shell and double-shell hybrid underwater vehicles model can be modelled in the software.
(2) Calculation section: For different types of underwater vehicles, target strength angle frequency spectrum, target strength variation curve with incident angle, and frequency response curve can be calculated. Taking the double-shell underwater vehicles as an example, the inner shell target strength, the outer shell target strength, and the total target strength of the underwater vehicles can be calculated. At the same time, an acoustic cover layer can be defined for the underwater vehicles and the calculation is the same as above.
(3) Post-processing section: The data can be exported to a designated folder, according to the requirements to further analyse the scattering characteristics of underwater vehicles.

The calculation parameters in the software include: calculation frequency, angle, and pitch angle. The calculation conditions include the type of underwater vehicles, whether to install the coated silent tiles or introduce reflection and transmission coefficients, etc.

Software features

(1) Taking full advantage of the 'MATLAB GUI' interface with excellent human-machine interaction, the software incorporates various coloured treatments for different underwater vehicles, enabling users to observe the entire modelling process.
(2) The software system defines the relative position parameters of the sub-targets, minimising user input requirements and keeping the modelling process fast and straightforward.
(3) The calculation data can be easily exported to a specified path as needed, streamlining calculations and saving time, thus simplifying subsequent processing.

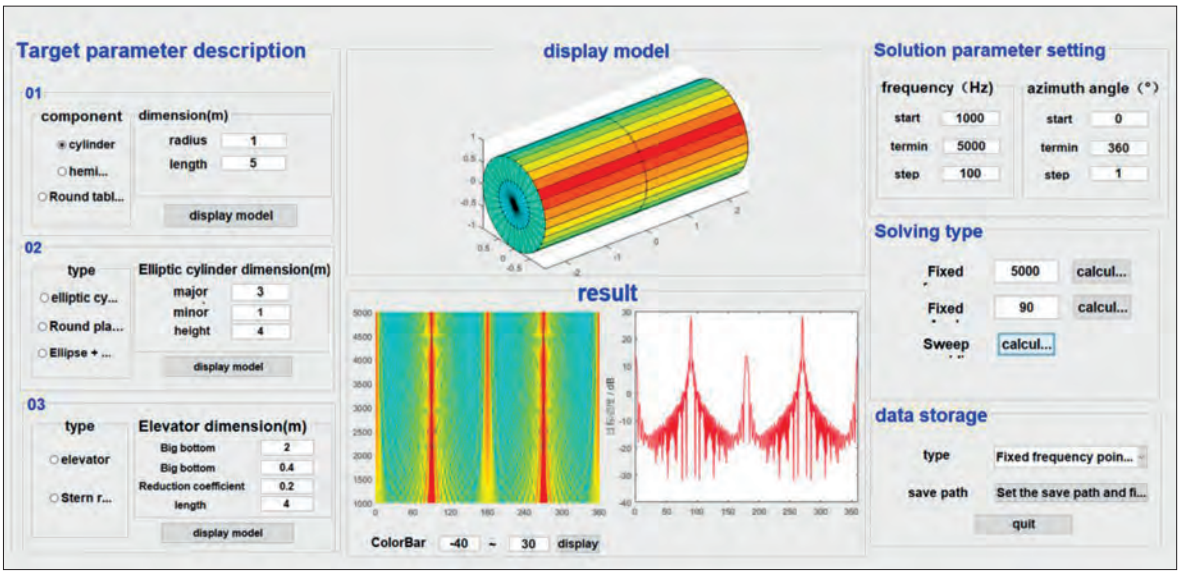

Fig. 15. Software demonstration interface

CONCLUSION

In this paper, the scattered sound field of a wedge-shaped structure is studied based on the modified highlight model. The highlight model of the wedge-shaped structure is finally obtained by calculating the trapezoidal plate through the 'segmentation-approximation-combination' method. The highlight models of other sub-structures of underwater vehicles are also calculated and the calculation results of the highlight model are compared with those of the planar element method.

The main conclusions are given as follows:

(1) It is important to choose an appropriate number of segments N when using the modified highlight model method. As the calculation frequency increases, N also needs to be increased appropriately. A small value of N will lead to a lack of precision, while a large value will lead to inefficient calculations.

(2) The modified highlight model method is highly consistent with the calculation results of the planar element method, in terms of changing trend and amplitude size, when it is used to calculate the angle frequency spectrum of sound target strength and the curve of sound target strength.

(3) For irregular targets, utilising a modified highlight model and taking into account the phase interference of different components can make the calculation results more accurate.

(4) The research results have certain engineering significance with the development of 'Target Strength Prediction Software for Simple Convex Structure of Underwater Vehicles' and 'Target Strength Fast Prediction Software for Multi-Highlight Interference of Underwater Vehicles'.

This research enriches the model library of highlight models and the developed software has high engineering significance, providing greater space for the prediction of underwater vehicles.

REFERENCES

1. W. Tang, J. Fan, and Z. Ma, 'Acoustic scattering of underwater target', Beijing: Science Press, 2018. (in Chinese)

2. Y. Sun, 'Wide-Frequency-Range prediction method of target strength of underwater structure and its application for submarine sails', Huazhong University of Science and Technology, 2019, doi: 10.27157/d.cnki.ghzku.2019.000843. (in Chinese)

3. H. Überall, R. Doolittle, and J. McNicholas, 'Use of sound pulses for a study of circumferential waves', The Journal of the Acoustical Society of America, vol. 39, no. 3, pp. 564-578, 1966, doi: 10.1121/1.1909929.

4. H. Zheng, R. Cai, and L. Pan, 'A modified Galerkin FEM for 1D Helmholtz equations', Applied Acoustics, vol. 74, no. 1, pp. 211-216, 2013, doi: 10.1016/j.apacoust.2012.06.014.

5. W. Murphy, V. Rokhlin, and M. Vassiliou, 'Solving electromagnetic scattering problems at resonance frequencies', Journal of Applied Physics, vol. 67, no. 10, pp. 6061-6065, 1990, doi: 10.1063/1.345217.

6. H. Schenck, 'Improved integral formulation for acoustic radiation problems', The Journal of the Acoustical Society of America, vol. 44, no. 1, pp. 41-58, 1968, doi: 10.1121/1.1911085.

7. H. Wu, L. Yu, and W. Jiang, 'A coupling FEM/BEM method with linear continuous elements for acoustic-structural interaction problems', Applied Acoustics, vol. 150, pp. 44-54, 2019, doi: 10.1016/j.apacoust.2019.02.001.

8. H. Li, Z. Lu, Y. Ke, Y. Tian, and W. Luo, 'A fast optimization algorithm of FEM/BEM simulation for periodic surface acoustic wave structures', Information, vol. 10, no. 3, p. 90, 2019, doi: 10.3390/info10030090.

9. W. Zhao, S. Marburg, and H. Chen, 'A FEM/BEM based topology optimization of submerged bi-material shell structures under harmonic excitations', INTER-NOISE and NOISE-CON Congress and Conference Proceedings, Institute of Noise Control Engineering, pp.763-774, 2018.

10. H. Chen and W. Zhao, 'A FEM/BEM based topology optimization of submerged bi-material shell structures under harmonic excitations', INTER-NOISE and NOISE-CON Congress and Conference Proceedings, Institute of Noise Control Engineering, pp. 5031-5015, 2017.

11. P. Waterman, 'Matrix theory of elastic wave scattering', The Journal of the Acoustical Society of America, vol. 60, no. 3, pp. 567-580, 1969, doi: 10.1121/1.381130.

12. F. Ingenito, 'Scattering from an object in a stratified medium', The Journal of the Acoustical Society of America, vol. 82, no. 6, pp. 2051-2059, 1987, doi: 10.1121/1.395649.

13. K. Lee and W. Seong, 'Time-domain Kirchhoff model for acoustic scattering from an impedance polygon facet', The Journal of the Acoustical Society of America, vol. 126, no. 1, pp. EL14-EL21, 2009, doi: 10.1121/1.3141887.

14. J. Fan, W. Tang, and L. Zhuo, 'Planar elements method for forecasting the echo characteristics from sonar targets', Journal of Ship Mechanics, vol. 16, no. Z1, pp.171-180, 2012. (in Chinese)

15. G. Zheng, J. Fan, and W. Tang, 'A modified planar elements method considering occlusion and secondary scattering', ACTA ACUSTICA, Chinese version, vol. 36, no. 04, pp. 377-383, 2011, doi: 10.15949/j.cnki.0371-0025.2011.04.010. (in Chinese)

16. W. Wang, B. Wang, J. Fan, and J. Zhou, 'An iterative planar elements method for calculating multiple acoustic scattering

from concave targets', Proceedings of the 18th Symposium on Underwater Noise of Ships, Wuxi: Key Laboratory of Ship Vibration and Noise, pp. 121-126, 2021, doi: 10.26914/c.cnkihy.2021.056714 . (in Chinese)

17. A. Abawi, 'Kirchhoff scattering from non-penetrable targets modeled as an assembly of triangular facets', The Journal of the Acoustical Society of America, vol. 140, no. 3, pp. 1878-1886, 2016, doi: 10.1121/1.4962735.

18. T. Stanton, 'Sound scattering by cylinders of finite length. I. Fluid cylinders', The Journal of the Acoustical Society of America, vol. 83, no. 1, pp. 55-62, 1988, doi: 10.1121/1.396184.

19. T. Stanton, 'Sound scattering by spherical and elongated shelled bodies', The Journal of the Acoustical Society of America, vol. 88, no. 3, pp. 1619-1633, 1990, doi: 10.1121/1.400321.

20. W. Tang, 'Highlight model of echoes from sonar targets', ACTA ACUSTICA, Chinese version , vol. 19, no. 2, pp. 92-100, 1994, doi: 10.15949/j.cnki.0371-0025.1994.02.002. (in Chinese)

21. W. Liu, J. Zhao, Y. Song, and J. Zhang, "Underwater target modelling technology based on modified highlight model", Torpedo Technology, vol. 18, no. 5, pp. 352-356, 2010. (in Chinese)

22. Y. Chen, "The research of target highlight modelling based on the planar elements clustering", China Ship Research and Development Academy, 2019. (in Chinese)

23. X. Zhang, J. Zhao, R. Wang, and J. Han, 'Modelling and simulation of scattering field for bistatic sonar', Journal of System Simulation, no. 5, pp. 562-565, 2002. (in Chinese)

24. C. Partridge and E. Smith, 'Acoustic scattering from bodies: Range of validity of the deformed cylinder method', The Journal of the Acoustical Society of America, vol. 97, no. 2, pp. 784-795, 1995, doi: 10.1121/1.412943.

25. J. Fan, 'Study on echo characteristics of underwater complex targets', Shanghai Jiao Tong University, 2001. (in Chinese)

26. Y. Guo, 'Nuclear submarine profile recognition', Ordnance Knowledge, no. 5, pp. 54-55, 2003, doi: 10.19437/j.cnki.11-1470/tj.2003.05.020. (in Chinese)

27. B. Li, 'Anti-active detection underwater target acoustic stealth shape optimization design', Jiangsu University of Science and Technology, 2020, doi: 10.27171/d.cnki.ghdcc.2020.000294. (in Chinese)